Amelioration of desmin network defects by αB-crystallin overexpression confers cardioprotection in a mouse model of dilated cardiomyopathy caused by LMNA gene mutation

Zoi Galata, Ismini Kloukina, Ioanna Kostavasili, Aimilia Varela, Constantinos H Davos, Manousos Makridakis, Gis le Bonne, Yassemi Capetanaki

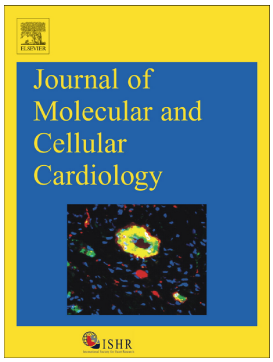

Amelioration of desmin network defects by Î±B-crystallin overexpression confers cardioprotection in a mouse model of dilated cardiomyopathy caused by LMNA gene mutation

Zoi Galata, Ismini Kloukina, Ioanna Kostavasili, Aimilia Varela, Constantinos H. Davos, Manousos Makridakis, GisÑ le Bonne, Yassemi Capetanaki

PII: S0022-2828(18)31057-5
DOI: doi:10.1016/j.yjmcc.2018.10.017
Reference: YJMCC 8834

To appear in: *Journal of Molecular and Cellular Cardiology*

Received date: 15 June 2018
Revised date: 2 October 2018
Accepted date: 16 October 2018

Please cite this article as: Zoi Galata, Ismini Kloukina, Ioanna Kostavasili, Aimilia Varela, Constantinos H. Davos, Manousos Makridakis, GisÑ le Bonne, Yassemi Capetanaki , Amelioration of desmin network defects by Î±B-crystallin overexpression confers cardioprotection in a mouse model of dilated cardiomyopathy caused by LMNA gene mutation. Yjmcc (2018), doi:10.1016/j.yjmcc.2018.10.017

Amelioration of desmin network defects by αB-crystallin overexpression confers cardioprotection in a mouse model of dilated cardiomyopathy caused by *LMNA* gene mutation

Zoi Galata[1], Ismini Kloukina[1], Ioanna Kostavasili[1], Aimilia Varela[2], Constantinos H. Davos[2], Manousos Makridakis[3], Gisèle Bonne[4] and Yassemi Capetanaki[1]*

[1]Center of Basic Research, [2]Center of Clinical, Experimental Surgery & Translational Research, [3]Center of Systems Biology, Biomedical Research Foundation, Academy of Athens, Athens 11527, Greece. [4]Sorbonne Université, INSERM UMRS-974, Center for Research in Myology, Institut de Myologie, G.H. Pitié Salpêtrière, F-75651 Paris Cedex 13, France.

* Corresponding author

Address correspondence to:
Yassemi Capetanaki,
Center of Basic Research,
Biomedical Research Foundation, Academy of Athens,
4 Soranou Ephesiou, Athens 11527, Greece
Telephone 30-210-6597212
Fax 30-210-6597212

Keywords: Cytoskeleton, desmin, lamin A/C, *LMNA* cardiomyopathy, αB-Crystallin.

Abstract

The link between the cytoplasmic desmin intermediate filaments and those of nuclear lamins serves as a major integrator point for the intracellular communication between the nucleus and the cytoplasm in cardiac muscle. We investigated the involvement of desmin in the cardiomyopathy caused by the lamin A/C gene mutation using the *Lmna*$^{H222P/H222P}$ mouse model of the disease. We demonstrate that in these mouse hearts desmin loses its normal Z disk and intercalated disc localization and presents aggregate formation along with mislocalization of basic intercalated disc protein components, as well as severe structural abnormalities of the intercalated discs and mitochondria. To address the extent by which the observed desmin network defects contribute to the progression of *Lmna*$^{H222P/H222P}$ cardiomyopathy, we investigated the consequences of desmin-targeted approaches for the disease treatment. We showed that cardiac-specific overexpression of the small heat shock protein αB-Crystallin confers cardioprotection in *Lmna*$^{H222P/H222P}$ mice by ameliorating desmin network defects and by attenuating the desmin-dependent mislocalization of basic intercalated disc protein components. In addition, αB-Crystallin overexpression rescues the intercalated discs, mitochondrial and nuclear defects of *Lmna*$^{H222P/H222P}$ hearts, as well as the abnormal activation of ERK1/2. Consistent with that, by generating the *Lmna*$^{H222P/H222P}$*Des+/-* mice, we showed that the genetically decreased endogenous desmin levels have cardioprotective effects in *Lmna*$^{H222P/H222P}$ hearts since less desmin is available to form dysfunctional aggregates. In conclusion, our results demonstrate that desmin network disruption, disorganization of intercalated discs and mitochondrial defects are a major mechanism contributing to the progression of this *LMNA* cardiomyopathy and can be ameliorated by αB-Crystallin overexpression.

1. Introduction

Cardiac muscle requires a high level of coordination between multiple cytoplasmic and nuclear components in order to function properly. This could be achieved by the cytoskeletal network of intermediate filaments (IFs), a fundamental cardiomyocyte structure with the potential to interact with numerous key elements involved in proper intracellular communication and mechanotransduction[1, 2]. More specifically, the continuous network formed by the IF proteins desmin and lamins provides a physical and functional coupling between the cytoplasm and the nuclear interior, either through the membrane spanning linkers of the nucleoskeleton to cytoskeleton complexes (LINC) or through nuclear pores[1-6].

Desmin is a key component of the three-dimensional IF cytoskeleton in striated muscle cells, which interlinks neighboring myofibrils at the level of Z discs and connects the whole myofibrillar apparatus with costameres, intercalated discs (IDs) as well as nuclei and mitochondria[1, 7]. A-type lamins consist of lamin A and C proteins (hereafter referred to as lamin A/C) which are encoded through alternative transcript splicing by the *LMNA* gene[8]. Lamin A/C together with B-type lamins are major components of the nuclear lamina, a highly organized lattice structure beneath the inner nuclear membrane[9]. Lamin proteins largely interact with proteins of the nucleoplasm and with chromatin, influencing numerous nuclear functions (e.g. DNA replication, RNA transcription and chromatin organization), extending their properties to the regulation of gene expression and transmission of signaling cascades[10, 11].

Interestingly, lamin A/C and desmin are among the most common IF proteins whose genetic mutations have been implicated in a number of familial cardiac pathologies such as dilated cardiomyopathy (DCM) and heart failure (HF) as well as skeletal myopathies[1, 2, 5, 12, 13]. Mutations on the *LMNA* gene are associated with more than 10 clinical pathologies, known as laminopathies, with DCM and skeletal myopathies being among the most common ones which can occur isolated or in association with disorders affecting other tissues[5, 12, 14]. On the other hand, dysfunctional desmin network due to desmin gene mutations or post-translational modifications (PTMs) causes a wide range of clinical and pathological manifestations, mainly hallmarked by abnormal desmin positive sarcoplasmic aggregates, which are collectively called desminopathies[2, 15-19]. Importantly, mutations in the small heat shock protein αB-Crystallin (αBCry) also cause desmin aggregate-related DCM and HF[1, 2, 20-22]. αBCry is the most abundant chaperone protein in the myocardium and among other functions, it interacts with desmin to prevent its abnormal aggregation and misfolding thus maintaining the cytoskeletal integrity[23-25]. In addition, recent data have revealed a potential interplay between desmin and αBCry in mitoprotection and cardioprotection[26] in a mouse model of DCM and HF with defects generated by desmin deficiency (*Des-/-*)[27-29].

Considering the continuous desmin-lamin cytoskeletal network and the finding that lamin A/C deficiency causes detachment of desmin from the nucleus[30, 31], we hypothesized that mutations in *LMNA* gene could probably negatively affect the desmin-lamin IF coupling leading to a disorganized and dysfunctional desmin network which, in turn, could further contribute to cardiomyocyte pathophysiology. Several transgenic mouse lines have been created to study the mechanisms implicated in *LMNA* cardiomyopathy[5]. Among them, the knock-in mouse carrying the H222P missense *Lmna* gene mutation serves as a useful animal model for the disease as it faithfully recapitulates the cardiac pathology that occurs in human subjects with *LMNA* mutations. The homozygous $Lmna^{H222P/H222P}$ mice develop DCM with increased myocardial fibrosis and defects in heart conduction system as well as muscular dystrophy[32]. Therefore using the $Lmna^{H222P/H222P}$ mice we sought to unveil a pathogenic role of desmin network defects in *LMNA* cardiomyopathy. We demonstrated that indeed in $Lmna^{H222P/H222P}$ hearts desmin loses its normal Z disk and ID localization pattern and presents intracytoplasmic localization and aggregate formation along with mislocalization of some basic ID protein components and severe ID and mitochondrial defects.

Furthermore, in order to reveal to what extent the desmin cytoskeletal defects contribute to the progression of *Lmna*$^{H222P/H222P}$ cardiomyopathy, we tried to develop ways to reduce or eliminate the desmin aggregates and investigate the consequences in disease development, thus concomitantly assessing if this strategy is a good target for both desminopathy and laminopathy treatment. We found that indeed the cardiac-specific overexpression of αBCry confers cardioprotection in *Lmna*$^{H222P/H222P}$ hearts by reducing desmin accumulation and aggregate formation and by attenuating all the above described ID and mitochondrial defects. The pathogenic role of desmin network defects in *LMNA* cardiomyopathy was further supported by the demonstration that reduction of endogenous desmin levels in *Lmna*$^{H222P/H222P}$*Des+/-* hearts leads to improvement of *Lmna*$^{H222P/H222P}$ cardiac pathology and function. The results herein allowed us to conclude that desmin network disruption and the consequences due to loss of normal desmin function and gain of toxic aggregate function, contribute to the development of this *LMNA* cardiomyopathy, a laminopathy with desminopathy characteristics that can be rescued by αBCry overexpression.

2. Materials and Methods

Detailed methods on breeding of mice, immunofluorescence, confocal microscopy, protein isolation, western blot, electron microscopy, immunogold labelling, RNA isolation and quantitative RT-PCR, 2-D gel electrophoresis, histology and transthoracic echocardiography can be found in the supplementary expanded method section.

2.1. Animals

Lmna$^{H222P/H222P}$ mice[32] were obtained from Dr. G. Bonne in a pure 129SV genetic background. Mice overexpressing of αBCry[26] and mice lacking desmin[29] had been generated and backcrossed on pure 129SV background (for at least 10 generations), as previously described. The *Lmna*$^{H222P/H222P}$αBCry and *Lmna*$^{H222P/H222P}$*Des+/-* mice were generated by crossing *Lmna*$^{H222P/H222P}$ mice with the two aforementioned mice categories. Details are provided in the online supplement.

2.2. Electron microscopy and immunogold labelling

For immunoelectron microscopy mice were sacrificed by cervical dislocation and transcardially perfused with cold fixative containing 4% Paraformaldehyde and 1% Glutaraldehyde in 0.1M PB (pH7.4). Hearts were rapidly dissected out, cut into 1mm cubes, post-fixed in the same fixative for 2hr and rinsed in 0.1M PB. Specimens were then dehydrated and embedded in Epon/Araldite resin mixture and allowed to polymerize at 60^{o}C for 24hr. Post-embedding immunogold labelling was performed on ultrathin sections from *Lmna*$^{H222P/H222P}$ mice hearts as previously described[33]. See online supplement for detailed protocol and antibodies.

2.3. Transthoracic echocardiography

Mice were anesthetized with intraperitoneal injection of 100 mg/kg Ketamine and situated in the supine position on a warming pad. 2-D targeted M-mode imaging was obtained to measure Left Ventricular (LV) End Diastolic and End Systolic Dimension (LVEDD and LVESD) and LV Posterior Wall thickness at systole and diastole (PWs and PWd). End diastole was determined at the maximal LV diastolic dimension and end systole was taken at the peak of posterior wall motion. The LV radius to PWT ratio (r/h) and the percentage of LV Fractional Shortening (FS [%] = [(EDD - ESD)/EDD] × 100) were also calculated, as previously described[34]. Three beats were averaged for each measurement. Echocardiographic experiments were performed using an ultrasound system (Vivid 7, GE healthcare) with a 13-MHz linear transducer. Images were analyzed using Echopac PC SW 3.1.3 software (GE healthcare).

2.4. Statistical analysis

Values are expressed as mean ± standard error (s.e.m.). Statistical analysis was performed using the appropriate method, ANOVA with Bonferroni-Dunn post-hoc test or Student's unpaired T-test along with Lavene's test for equality of variances, as indicated in each case. Statistical comparisons and graphs were performed using SPSS 22.0 (IBM Corp.) or using StatView 5.0 (Abacus Concepts) for the analysis of echocardiographic measurements. A value of $p<0.05$ was considered statistically significant.

3. Results

3.1. Desmin loses its normal localization and exhibits intracytoplasmic aggregate deposition accompanied by mislocalization of basic ID protein components in *Lmna*$^{H222P/H222P}$ hearts.

We studied the effects of *LMNA* mutation on desmin morphology and localization and potential structural consequences by immunofluorescence microscopy on *Lmna*$^{H222P/H222P}$ heart sections. Female *Lmna*$^{H222P/H222P}$ mice develop signs and symptoms of the disease pathology at significantly later ages[32], therefore, we used for our experiments only male *Lmna*$^{H222P/H222P}$ mice at the age of 20-weeks. We observed that in *Lmna*$^{H222P/H222P}$ hearts desmin loses its normal Z disk and ID staining pattern and presents a significant cytoplasmic aggregate deposition within the cardiomyocytes (Fig. 1A, S3Ba). Furthermore, we examined some major protein components of the IDs and we revealed that they exhibit a disorganized pattern. Specifically, we studied desmoplakin and plakoglobin as basic components of the ID desmosome-adherens junction combined structures termed "area composita"[35, 36]. We found that desmoplakin, the direct desmin-binding partner and central protein component of desmosomes, is severely mislocalized showing cytoplasmic localization with a diffused dot-like staining pattern under confocal microscopy (Fig. 2Aa-b, S3Bb). On the other hand, plakoglobin, a basic protein component of the IDs found in both fascia adherens junctions (sites that anchor actin cytoskeleton) and desmosomes, although it presents also an abnormal localization pattern, it does not exhibit very severe cytoplasmic accumulation in cardiomyocytes but it rather shows a lateral localization (Fig. S3Aa-b,Bc). Furthermore, connexin-43, the major gap junction protein component of the IDs displays a severely disorganized staining pattern with abnormal intracellular localization that results in an obvious punctate staining within the cytoplasm (Fig. 2Ba-b, S3Bd). Interestingly, the above mentioned intracellular localization of ID proteins does not seem to exhibit an apparent co-localization with desmin cytoplasmic deposition within the *Lmna*$^{H222P/H222P}$ cardiomyocytes, with the exception of connexin-43 which shows some but not extended co-localization.

3.2. *Lmna*$^{H222P/H222P}$ cardiac muscle exhibits severe ID and mitochondrial ultrastructural defects.

The analysis of *Lmna*$^{H222P/H222P}$ cardiac muscles by electron microscopy confirmed the formation of amorphous aggregates and the ID abnormalities described above, and further revealed extensive ultrastructural mitochondrial defects (Fig. 1B). The aggregates, constituted mainly by filamentous-like material and membranous remnants, are localized between disturbed myofibrils and mitochondria (Fig. 1Ba), around the nuclei (Fig. 1Bb,d) and in the vicinity of defected IDs (Fig. 1Bc,e-f). The presence of desmin inside the aggregates was further confirmed by immunogold labelling (Fig. 1Baa′). The IDs are severely affected, showing a disorganized and stretched pattern. They present lacunae and regions in which the myofibrils appear to be completely disconnected either on one or sometimes on both attachment sites of the IDs (Fig. 1Bc,e-f). Mitochondrial defects include aberrant shape and distribution (Fig. 1Ba-b), degeneration with disrupted cristae (Fig. 1Bb,d), fragmentation and abnormal accumulation (Fig. 1Bd-f), mainly in cardiomyocytes with severe aggregate formation, as expected (Fig. 1Ba-f). The nuclei of the cardiomyocytes present the characteristic elongated shape (Fig. 1Bc, S1Bd), with less apparent compact heterochromatin (Fig. 1Bc), occasionally dilation of the intermembrane space and destroyed membrane (Fig. 1Bd, S1Ba), as well as other nuclear shape abnormalities (Fig. S1B).

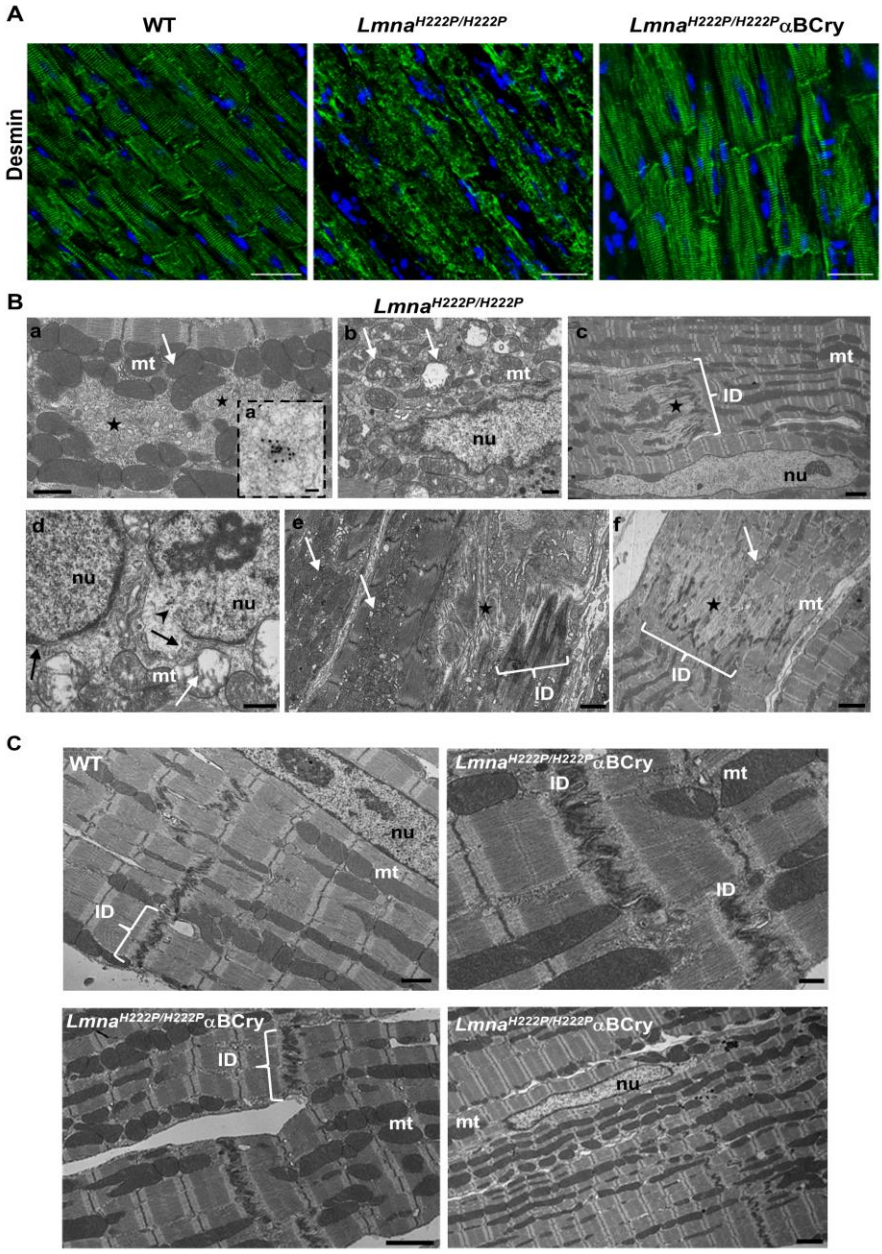

Fig.1. *Lmna*$^{H222P/H222P}$ cardiac muscle is characterized by desmin aggregate formation, structural ID abnormalities and mitochondrial defects (A,B), most of which are ameliorated by αBCry overexpression in *Lmna*$^{H222P/H222P}$αBCry hearts (A,C). Representative immunofluorescence images of myocardial cryosections after immunostaining for desmin (green) (**A**). Nuclei are counterstained blue with Hoechst (N=8 for each genotype). Electron microscopic images of *Lmna*$^{H222P/H222P}$ (N=5) (**Ba**-**f**), *Lmna*$^{H222P/H222P}$αBCry (N=3) and WT (N=3) heart tissues (**C**). Cytoplasmic aggregates are pointed with asterisks (**Ba**,**c**,**e**-**f**) and defected IDs are pointed with brackets (**Bc**,**e**-**f**). Immunogold labelling for desmin at aggregate containing areas, similar to the indicated by asterisks in Ba, is shown in the square (**Baa´**). The nuclei of the *Lmna*$^{H222P/H222P}$ cardiomyocytes present the characteristic abnormal elongation with less apparent compact heterochromatin (**Bc**). Dilation of the nuclear intermembrane space is pointed with black arrows and rupture of the inner nuclear membrane is indicated with arrowhead (**Bd**). Multiple mitochondrial defects, including abnormal shape, size and positioning (**Ba**-**b**), degeneration with disrupted cristae (**Bb**,**d**), fragmentation and abnormal accumulation (**Bd**-**f**), are indicated by white arrows. Both ID and mitochondrial defects are present predominantly in areas with severe aggregate formation. The mice from all genotypes were male at the age of 20-weeks. Scale bars: 25μm (**A**), 1μm (**C**(WT),**Ba**,**e**), 2μm (**Bc**,**f**,**C**(*Lmna*$^{H222P/H222P}$αBCry lower panel)), 50nm (**Baa´**), 500nm (**Bb**,**d**,**C**(*Lmna*$^{H222P/H222P}$αBCry upper panel)). mt: mitochondria, nu: nucleus.

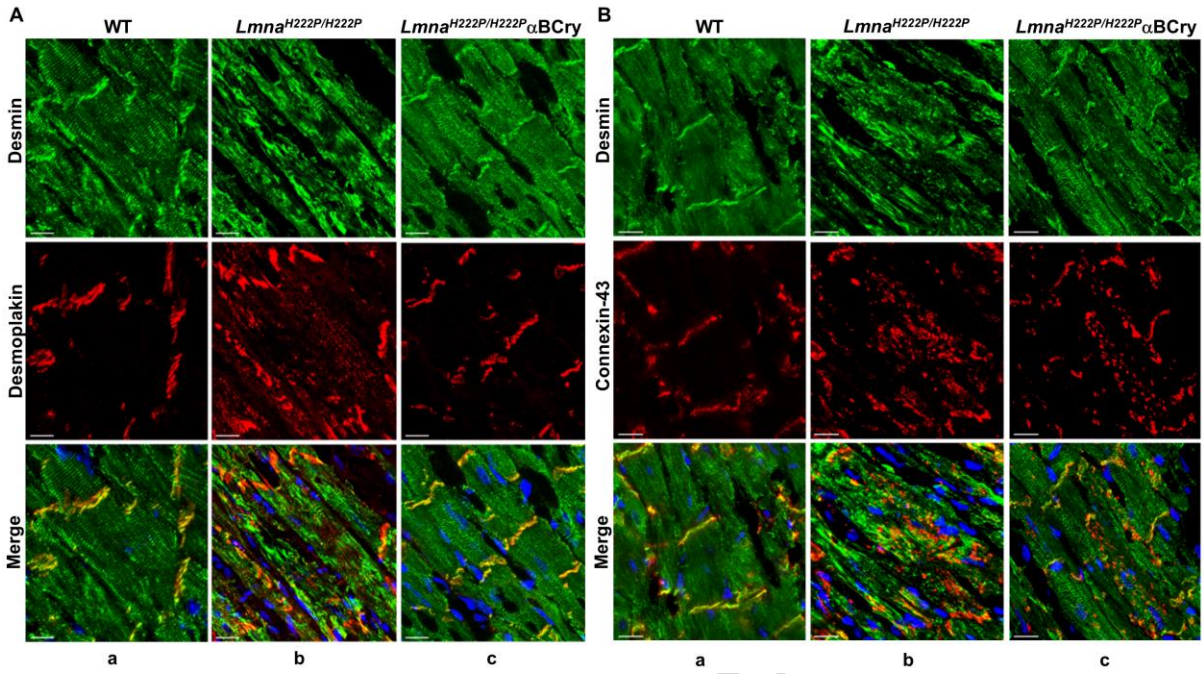

Fig.2. Desmin network defects and mislocalization of the ID proteins desmoplakin and connexin-43 in *Lmna*$^{H222P/H222P}$ hearts are significantly attenuated in *Lmna*$^{H222P/H222P}$αBCry hearts. Representative images of myocardial cryosections from 20 wk-old male mice after double immunofluorescence staining for desmin (green) and desmoplakin (**A**) or connexin-43 (**B**) (red) (N=8 animals for each genotype). Scale bars: 25μm.

3.3. Alterations in desmin protein levels and post-translational modifications (PTMs) in *Lmna*$^{H222P/H222P}$ hearts.

In order to get some insight on the mechanism by which the *LMNA* mutation causes desmin aggregate formation we investigated desmin levels and potential PTMs. We analyzed by Western blot the protein levels of desmin along with its mRNA expression in *Lmna*$^{H222P/H222P}$ hearts. We demonstrated that desmin protein exhibits a 5.6 fold increase in *Lmna*$^{H222P/H222P}$ hearts compared to WT (Fig. 3A-B). The elevated protein levels do not reflect a precedent upregulation in desmin mRNA levels as demonstrated by RT-PCR analysis (Fig. 3C). We next performed 2-Dimensional (2-D) gel electrophoresis in total protein extracts from *Lmna*$^{H222P/H222P}$ hearts followed by immunoblot for desmin in order to check its PTM status. The results indicated that desmin appears not only more abundant in *Lmna*$^{H222P/H222P}$ hearts but it presents also some more acidic isoforms that suggest a higher phosphorylation status (Fig. 3D-E). This might explain the desmin accumulation and aggregate formation in these cardiomyocytes, as desmin hyper-phosphorylation can cause filament disassembly[37-40] and aggregate formation that could also affect the normal turnover of the protein.

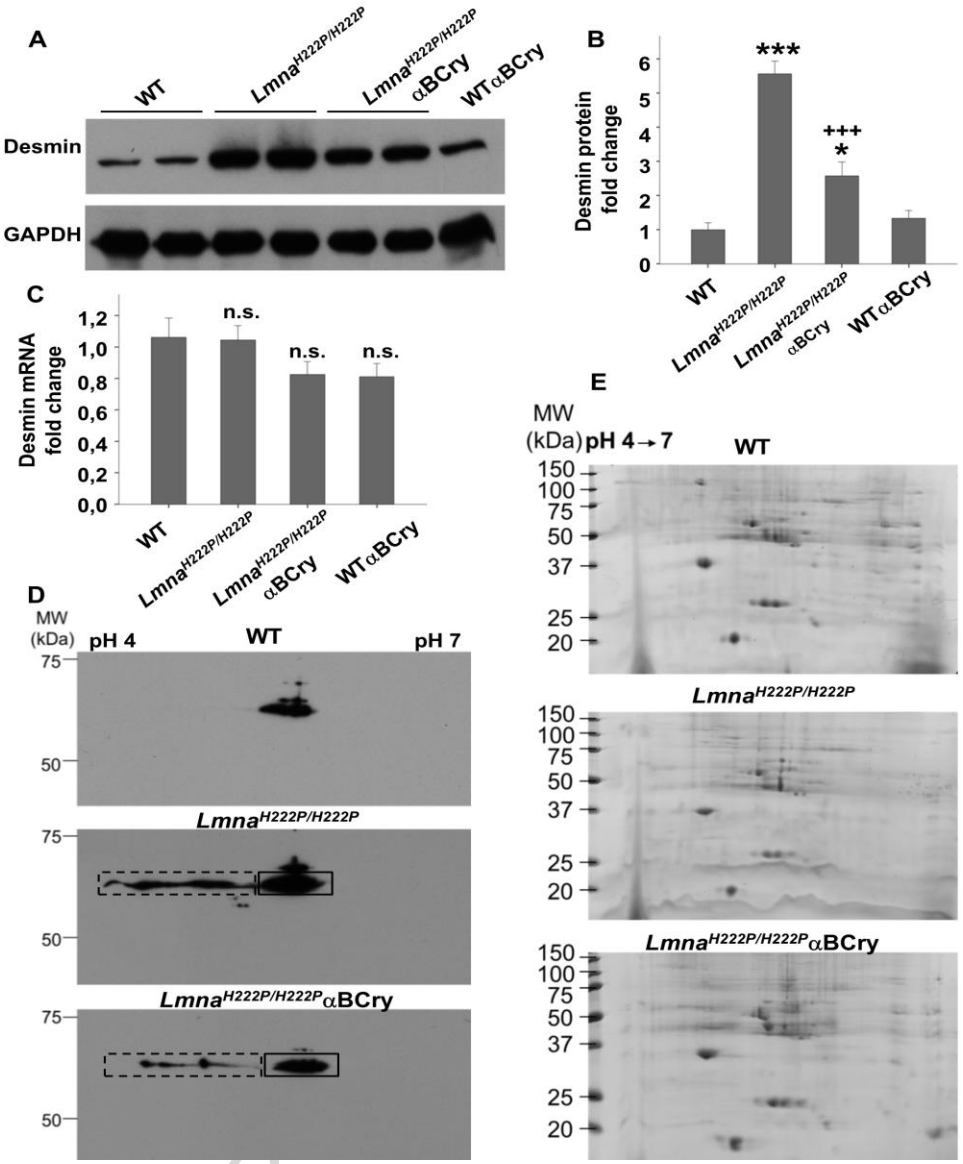

Fig.3. Desmin increase and PTM changes in *Lmna*$^{H222P/H222P}$ hearts. αBCry cardiac overexpression attenuates the elevated desmin protein levels and reduces the proportion of desmin with increased PTMs in *Lmna*$^{H222P/H222P}$ hearts. Western blot analysis for desmin in whole heart lysates (**A**). Increased desmin protein levels in *Lmna*$^{H222P/H222P}$ hearts (5.6 fold change vs WT) are significantly attenuated in *Lmna*$^{H222P/H222P}$ αBCry hearts (2.6 fold change vs WT) (N=8 for WT, *Lmna*$^{H222P/H222P}$ and N=7 for *Lmna*$^{H222P/H222P}$ αBCry, WTαBCry) (**B**). RT-PCR experiments with mRNA from total hearts revealed almost equal desmin expression levels in all mouse genotypes (N=8 for WT, N=6 for *Lmna*$^{H222P/H222P}$ and N=5 for *Lmna*$^{H222P/H222P}$ αBCry, WTαBCry) (**C**). Western blot analysis with desmin antibody in heart protein extracts after 2-D gel electrophoresis (first dimension pH4-7 IPG strips followed by second dimension 12% SDS-PAGE). The more acidic shift of desmin in *Lmna*$^{H222P/H222P}$ and *Lmna*$^{H222P/H222P}$ αBCry hearts is indicated with dashed rectangles and the main desmin band with black rectangles (N=3 for WT and N=4 for *Lmna*$^{H222P/H222P}$, *Lmna*$^{H222P/H222P}$ αBCry). Quantification of desmin bands of *Lmna*$^{H222P/H222P}$ and *Lmna*$^{H222P/H222P}$ αBCry 2-D blots revealed that phosphorylated desmin (dashed rectangles) consists approximately 66.9% and 38.4% of the main desmin band (black rectangles) respectively (**D**). Representative 2-D gels stained with Colloidal Coomassie Blue similar to those used for Western blot in order to check the equal protein loading (**E**). 20 wk-old male mice were used in all cases. Error bars: ± s.e.m. Data were analyzed pairwise with Student's unpaired T-test ***p<0.001 vs WT or WT αBCry; *p<0.05 vs WT or WT αBCry; $^{+++}$p<0.001 vs *Lmna*$^{H222P/H222P}$; n.s.: not statistically significant.

3.4. αB-Crystallin (αBCry) overexpression in *Lmna*$^{H222P/H222P}$ hearts ameliorates abnormal desmin localization and aggregate formation and improves heart function.

In an effort to investigate to what extent the desmin cytoskeletal defects contribute to the progression of *LMNA* cardiomyopathy, we generated *Lmna*$^{H222P/H222P}$ mice overexpressing αBCry in the heart by crossing the *Lmna*$^{H222P/H222P}$ mice with transgenic mice line that has cardiac-specific overexpression of αBCry driven by the α-myosin heavy chain (α-MHC) promoter[41]. The generated and studied mice were homozygotes for the H222P mutation in *Lmna* gene and heterozygotes for the transgene of αBCry overexpression, simply referred to as the *Lmna*$^{H222P/H222P}$αBCry mice. As indicated by Western blot analysis of total heart lysates, *Lmna*$^{H222P/H222P}$ mice exhibit a slight increase in the expression of the endogenous αBCry compared to WT (1.4 fold change) while the transgenic lines *Lmna*$^{H222P/H222P}$αBCry and WTαBCry present a 6 fold and 5.6 fold increase of αBCry protein levels respectively (Fig. 4A-B).

To examine a potential cardioprotective role of the overexpressed αBCry in *Lmna*$^{H222P/H222P}$ mice, we evaluated through 2D-directed M-mode echocardiography the heart function of *Lmna*$^{H222P/H222P}$αBCry mice. We found that the heart function of *Lmna*$^{H222P/H222P}$αBCry mice is significantly improved compared to *Lmna*$^{H222P/H222P}$ as indicated by the increased percentage (~30%) of Fractional Shortening (FS) (Fig. 5E and Table 1). Furthermore, all the additional cardiac parameters such as the Left Ventricular (LV) End Diastolic and End Systolic Dimension (LVEDD and LVESD), the LV Posterior Wall thickness at diastole and systole (PWd or PWs) and the r/h ratio are also considerably improved (Table 1).

Confocal microscopy in *Lmna*$^{H222P/H222P}$ heart sections revealed a strong co-localization of the endogenous αBCry with desmin aggregates (Fig. 4C). This is in agreement with the well-established role of αBCry as a chaperone protein and its ability to interact with desmin and prevent its misfolding and aggregation[23-25]. Most importantly, overexpression of αBCry in *Lmna*$^{H222P/H222P}$ cardiomyocytes led to extensive decrease in desmin accumulation and aggregate formation (Fig. 2Ac,Bc, S3Ac) and restored proper localization of desmin at Z disks and IDs. Consistent with that, desmin protein levels are reduced as shown by immunoblot analysis (Fig. 3A-B). In addition, 2-D Western blot analysis of heart extracts from *Lmna*$^{H222P/H222P}$αBCry mice revealed a decrease (~50%) in the desmin PTM status relative to *Lmna*$^{H222P/H222P}$, suggesting that the overexpression of αBCry acts by preventing both aberrant PTMs and aggregate formation (Fig. 3D-E).

Table 1. Echocardiographic measurements of *Lmna*$^{H222P/H222P}$ and *Lmna*$^{H222P/H222P}$ αBCry male mice at the age of 20 weeks together with WT and WTαBCry controls matching on age and gender.

	WT	*Lmna*$^{H222P/H222P}$	*Lmna*$^{H222P/H222P}$αBCry	WTαBCry
n	13	18	16	10
FS (%)	44.49±0.91***+++	26.90±1.07	34.98±0.99***	43.85±0.73***+++
LVEDD (mm)	3.73±0.10**	4.09±0.07	3.79±0.07*	3.72±0.12**
LVESD (mm)	2.08±0.08***++	2.99±0.09	2.48±0.08***	2.09±0.08***++
LVPWd (mm)	0.76±0.01***++	0.64±0.01	0.71±0.01***	0.75±0.01***+
LVPWs (mm)	1.28±0.01***+++	1.06±0.02	1.17±0.01***	1.28±0.01***+++
r/h	2.46±0.10***	3.21±0.09	2.67±0.08***	2.49±0.12
HR (bpm)	547.83±19.77***+	449.37±10.28	501.15±12.74*	547.53±22.37***+

Means ± s.e.m.; Fractional Shortening (FS); Left Ventricular End Diastolic or Systolic Dimension (LVEDD, LVESD); Left Ventricular Posterior Wall thickness at diastole or systole (LVPWd, LVPWs);

Ratio of LV radius to PWT (r/h). Data were analyzed with ANOVA with Bonferroni-Dunn post-hoc test *p<0.05, **p<0.01, ***p<0.0001 vs *Lmna*$^{H222P/H222P}$; +p<0.05, ++p<0.01, +++p<0.0001 vs *Lmna*$^{H222P/H222P}$ αBCry.

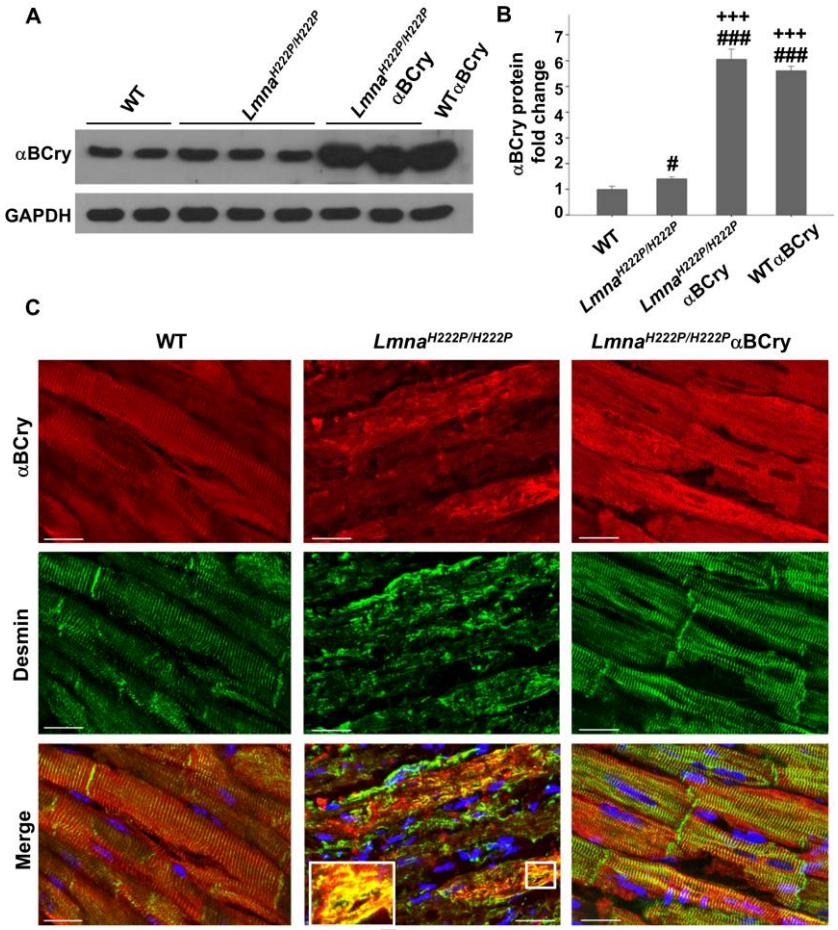

Fig.4. αBCry overexpression in *Lmna*$^{H222P/H222P}$ hearts ameliorates abnormal desmin localization and aggregate formation. Western blot analysis for αBCry protein in total heart lysates. GAPDH was used as loading control (**A**). Quantification of αBCry protein levels (N=7 for *Lmna*$^{H222P/H222P}$ and N=5 for WT, *Lmna*$^{H222P/H222P}$ αBCry, WTαBCry) (**B**). Immunofluorescence analysis of myocardial cryosections after double staining with antibodies against desmin (green) and αBCry (red). The nuclei were counterstained blue with Hoechst (N=6 for each genotype) (**C**). A higher magnification image of the indicated boxed area emphasizes the colocalization of αBCry with desmin aggregates in *Lmna*$^{H222P/H222P}$ hearts. 20 wk-old male mice were used in all cases. Error bars: ± s.e.m. Data were analyzed pairwise with Student's unpaired T-test $^{+++}$p<0.001 vs *Lmna*$^{H222P/H222P}$; $^{###}$p<0.001 vs WT; $^{#}$p<0.05 vs WT. Scale bars: 25μm.

3.5. Overexpression of αBCry attenuates mislocalization of additional ID protein components and rescues the ultrastructural defects of cardiac muscle in *Lmna*$^{H222P/H222P}$ mice.

In order to determine whether the extensive reduction of desmin aggregates and mislocalization could restore the proper localization of other ID components, we performed additional immunofluorescence microscopy on *Lmna*$^{H222P/H222P}$αBCry heart sections. We demonstrated that in *Lmna*$^{H222P/H222P}$αBCry hearts desmin is properly co-localized at IDs with other ID proteins including desmoplakin, plakoglobin and connexin-43 (Fig. 2Ac,Bc, S3Ac,Ba). In parallel, the cytoplasmic mislocalization of desmoplakin, plakoglobin and connexin-43 found in *Lmna*$^{H222P/H222P}$ hearts is significantly reduced in *Lmna*$^{H222P/H222P}$αBCry cardiomyocytes (Fig. S3Bb-d). Desmoplakin exhibits the most significant restoration of proper ID localization pattern (Fig. 2Ac, S3Bb) while connexin-43 exhibits a partial restoration as part of its abnormal cytoplasmic punctate staining pattern is still visible in *Lmna*$^{H222P/H222P}$αBCry hearts (Fig. 2Bc, S3Bd). The control immunofluorescence experiments in hearts from WTαBCry mice verified that the αBCry overexpression does not have any

obvious effects in the localization pattern of the aforementioned ID protein components (Fig. S4). These results indicate that the observed rearrangements of the ID protein components in *Lmna*$^{H222P/H222P}$αBCry mice hearts occur in a desmin-dependent fashion, which affects mainly the direct desmin-binding partners such as desmoplakin. Electron microscopy analysis of *Lmna*$^{H222P/H222P}$αBCry cardiac muscles showed that the overexpressed αBCry rescues extensively the ultrastructural defects of *Lmna*$^{H222P/H222P}$ heart tissue. Specifically, the presence of amorphous aggregates in *Lmna*$^{H222P/H222P}$αBCry cardiac muscles is markedly decreased, the IDs demonstrate a properly organized pattern without lacunae or other structural abnormalities and mitochondria look indeed like wild type (Fig. 1C).

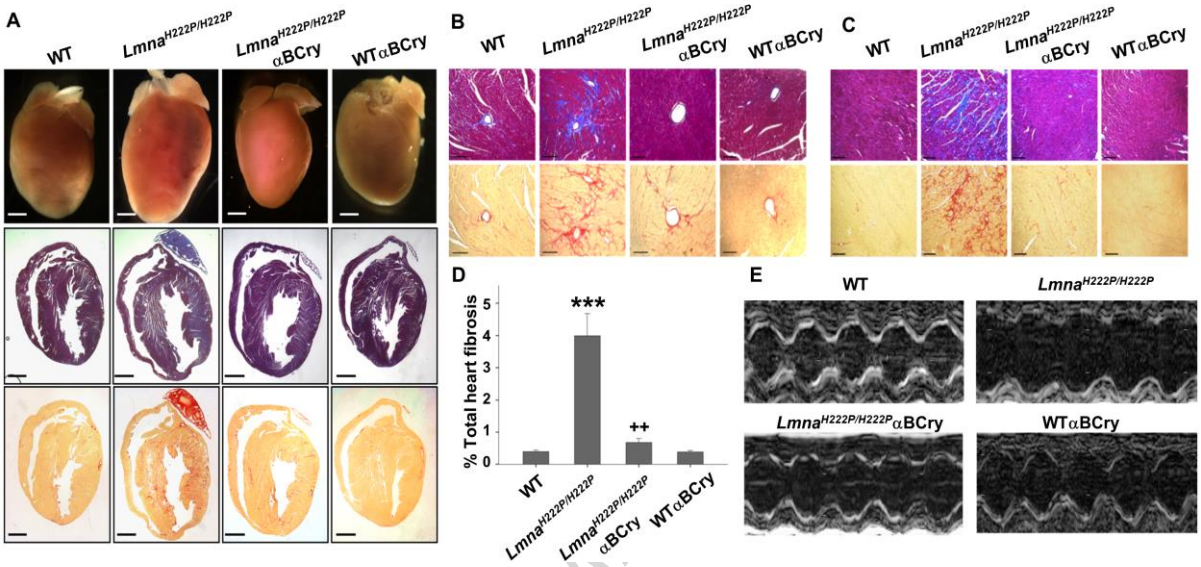

Fig.5. αBCry overexpression ameliorates myocardial remodeling and dilation and improves heart function in *Lmna*$^{H222P/H222P}$ hearts. Whole hearts from WT, *Lmna*$^{H222P/H222P}$, *Lmna*$^{H222P/H222P}$αBCry and WTαBCry mice (first line) or sections of paraffin-embedded heart tissues after staining with Masson's trichrome (second line) or picrosirius red dye (third line) (**A**). Representative bright field images from heart sections stained with Masson's trichrome (first line) or picrosirius red (second line), indicating the heart areas with perivascular (**B**) or interstitial (**C**) fibrosis and quantification of total fibrosis (%index) (N=8 for each genotype) (**D**). Characteristic pictures from 2D-directed M-mode echocardiographic tracings (**E**). 20 wk-old male mice were used in all cases. Error bars: ± s.e.m. Data were analyzed pairwise with Student's unpaired T-test ***p<0.001 vs WT or WTαBCry; $^{++}$p<0.01 vs *Lmna*$^{H222P/H222P}$. Scale bars: 1mm (**A**), 50μm (**B**-**C**).

3.6. Cardiac overexpression of αBCry in *Lmna*$^{H222P/H222P}$ mice reduces significantly the heart fibrosis, the abnormal nuclear elongation of cardiomyocytes and the aberrant activation of ERK1/2.

To further examine the effects of the αBCry overexpression in *Lmna*$^{H222P/H222P}$ heart defects, we investigated some of the most well-documented pathological features of *Lmna*$^{H222P/H222P}$ mice such as the increased cardiac fibrosis[32, 42], the abnormally elongated nuclei of cardiomyocytes[32, 43] and the increased activation of ERK1/2 (extracellular signal-regulated kinase 1/2) signaling pathway[43-45]. We demonstrated that in *Lmna*$^{H222P/H222P}$αBCry hearts the amount of total fibrosis which is either present at perivascular and/or at interstitial areas of the heart, is markedly reduced (Fig. 5A-D), compared to *Lmna*$^{H222P/H222P}$. Additionally, the mean nuclear length of cardiomyocytes is significantly decreased reaching almost the levels of the WT mice (Fig. 6A-C). We also revealed that the overexpression of αBCry in *Lmna*$^{H222P/H222P}$ myocardium results in a significant reduction of the ERK1/2 abnormal activation, as indicated by immunoblot analysis in protein extracts from *Lmna*$^{H222P/H222P}$αBCry hearts in which the phosphorylated ERK1/2 to total ERK1/2 ratios are reduced significantly compared to *Lmna*$^{H222P/H222P}$ (Fig. 6D-E).

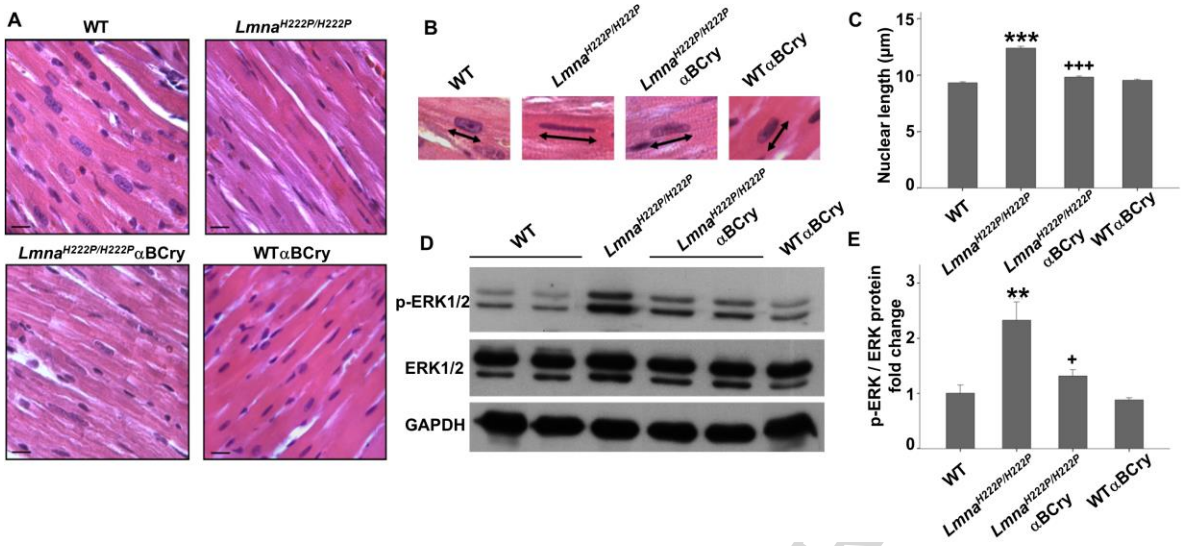

Fig.6. Abnormal nuclear length and ERK1/2 activation in *Lmna*$^{H222P/H222P}$ hearts are rescued by αBCry cardiac overexpression. Representative bright field microscopy images of paraffin-embedded heart sections after staining with hematoxylin/eosin dyes (**A**). Characteristic nuclei of cardiomyocytes from different genotypes with their length depicted with arrows (**B**). Quantification of the nuclear length of cardiomyocytes with ImageJ software (total 800 well-defined nuclei were measured in N=8 animals from each genotype) (**C**). Western blot analysis with antibodies against phospho-ERK1/2 (p-ERK1/2) and total ERK1/2 proteins in total heart lysates (**D**). Quantification of ERK1/2 activation (normalized to the WT levels) by measuring the ratio of pERK1/2 to total ERK1/2 protein levels (N=8 for WT, N=6 for *Lmna*$^{H222P/H222P}$, *Lmna*$^{H222P/H222P}$ αBCry and N=5 for WTαBCry) (**E**). 20 wk-old male mice were used in all cases. Error bars: ± s.e.m. Data were analyzed pairwise with Student's unpaired T-test ***p<0.001 vs WT or WTαBCry; **p<0.01 vs WT or WTαBCry; $^{+++}$p<0.001 vs *Lmna*$^{H222P/H222P}$; $^{+}$p<0.05 vs *Lmna*$^{H222P/H222P}$. Scale bars: 10μm (**A**).

3.7. *In vivo* reduction of endogenous desmin levels in *Lmna*$^{H222P/H222P}$*Des+/-* hearts decreases desmin abnormal aggregation, restores the proper localization of desmin and other ID proteins and markedly improves cardiac function.

In an effort to assess further the importance of desmin network disruption and aggregate formation in the *Lmna*$^{H222P/H222P}$ cardiomyopathy, we attempted to genetically decrease the endogenous desmin levels, considering that this would respectively decrease the aggregates and consequently their toxic effect. For this purpose, we generated *Lmna*$^{H222P/H222P}$*Des+/-* mice, by crossing *Lmna*$^{H222P/H222P}$ with *Des-/-* mice, and confirmed the expression of 50% of the WT desmin levels (Fig. S5).

The analysis of male *Des+/-* mice by 2D-directed M-mode echocardiography at the age of 20-weeks indicated that they maintain an adequate cardiac function despite the 50% reduction of the endogenous desmin protein levels (Table S1). Similar analysis with *Lmna*$^{H222P/H222P}$*Des+/-* male mice at the same age demonstrated that their cardiac function is improved significantly, as indicated by the increased percentage (~39%) of FS compared to that of *Lmna*$^{H222P/H222P}$ hearts (Fig. 7D and Table S1).

We next analyzed by immunoblotting the levels of desmin in *Lmna*$^{H222P/H222P}$*Des+/-* hearts and we found that they are reduced significantly compared to *Lmna*$^{H222P/H222P}$ (Fig. 7A-B). The 5.6 fold desmin increase in *Lmna*$^{H222P/H222P}$ hearts drops to 3.3 fold in *Lmna*$^{H222P/H222P}$*Des+/-* hearts (change vs WT). In line with that, the lower levels of endogenous desmin in *Lmna*$^{H222P/H222P}$*Des+/-* hearts ameliorate the abnormal desmin intracytoplasmic accumulation and aggregate formation, as indicated by immunofluorescence analysis (Fig. 7C).

To address the effects of the decreased endogenous desmin protein levels on the *Lmna*$^{H222P/H222P}$ cardiomyocyte organization, we examined by confocal microscopy the localization pattern of desmin, desmoplakin, plakoglobin and connexin-43 in

Lmna$^{H222P/H222P}$*Des+/-* hearts. We revealed that in these mouse hearts desmin localizes properly at the Z disks and IDs. Consistent with that, desmoplakin and plakoglobin exhibit also a properly organized staining pattern and co-localize with desmin at the IDs (Fig. 7Ca-b). However, the mislocalization of the gap junction protein connexin-43 seems to be partially attenuated (Fig. 7Cc).

3.8. The reduced endogenous desmin levels of *Lmna*$^{H222P/H222P}$*Des+/-* mice restrict the abnormal activation of ERK1/2 but they do not affect significantly the amount of total heart fibrosis.

To further investigate the mechanisms by which the reduction of the endogenous desmin protein levels in *Lmna*$^{H222P/H222P}$ mice has cardioprotective role, we examined the activation of ERK1/2 signaling pathway in *Lmna*$^{H222P/H222P}$*Des+/-* hearts (Fig. 7E-F). We demonstrated that there is a significant reduction of the ERK1/2 activation in *Lmna*$^{H222P/H222P}$*Des+/-* hearts compared to *Lmna*$^{H222P/H222P}$. However, the analysis and quantification of total heart fibrosis revealed that the reduced endogenous desmin levels of *Lmna*$^{H222P/H222P}$*Des+/-* mice do not affect significantly the total heart fibrosis compared to *Lmna*$^{H222P/H222P}$, although we observe a trend of decline (Fig. S6).

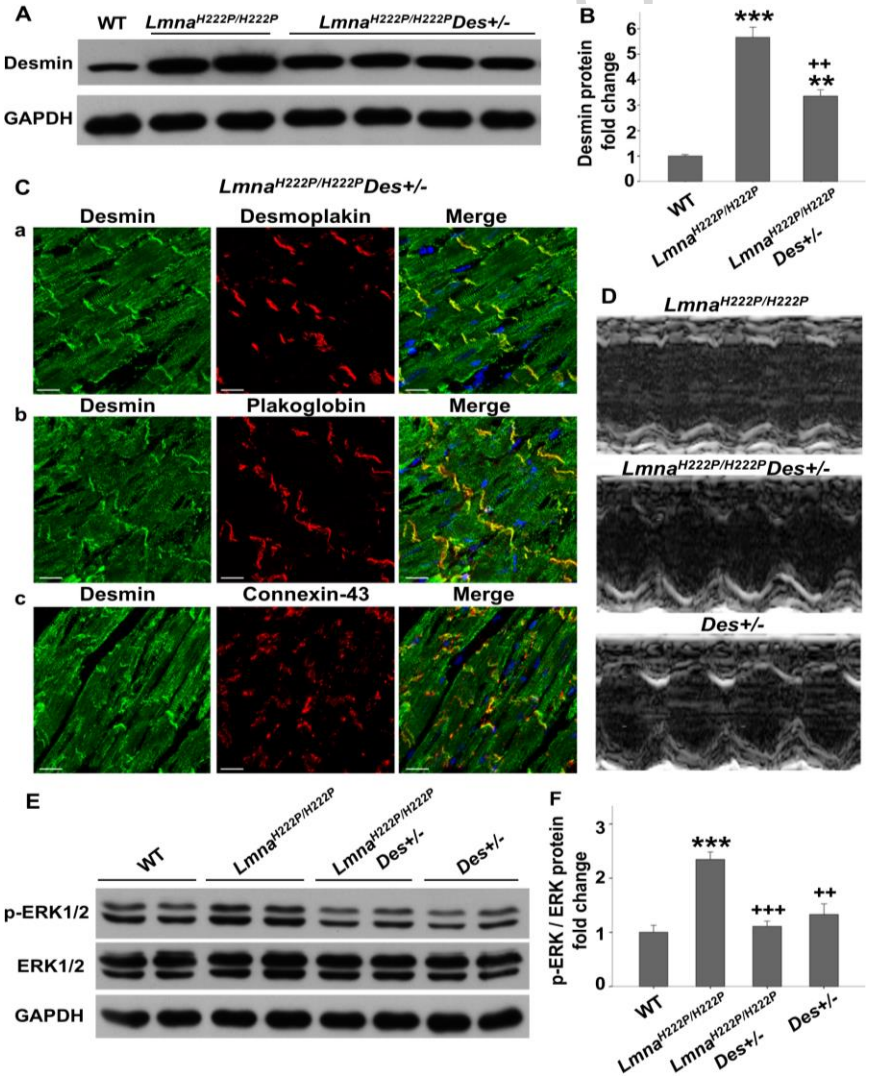

Fig.7. Decrease in endogenous desmin levels in *Lmna*$^{H222P/H222P}$*Des+/-* hearts decreases aggregate formation, restores proper localization of ID protein components, decreases abnormal ERK1/2 activation and improves cardiac function. Western blot analysis for desmin in whole heart lysates. GAPDH was used as loading control (**A**). The 5.6 fold desmin increase in

Lmna$^{H222P/H222P}$ hearts drops to 3.3 fold in *Lmna*$^{H222P/H222P}$ *Des*+/- hearts (change vs WT) (N=7 for *Lmna*$^{H222P/H222P}$ and N=6 for WT and *Lmna*$^{H222P/H222P}$, N=5 for *Lmna*$^{H222P/H222P}$ *Des*+/-) (**B**). Immunofluorescence analysis of myocardial cryosections from *Lmna*$^{H222P/H222P}$ *Des*+/- hearts after double immunofluorescence staining with antibodies against desmin (green) and desmoplakin, plakoglobin or connexin-43 (red). The nuclei were counterstained blue with Hoechst (**C**). Characteristic pictures from 2D-directed M-mode echocardiographic tracings (**D**). Western blot analysis with antibodies against phospho-ERK1/2 (p-ERK1/2) and total ERK1/2 proteins in total heart lysates (**E**). Quantification of ERK1/2 activation (normalized to WT levels) by measuring the ratio of pERK1/2 to total ERK1/2 protein levels (N=4 for each genotype) (**F**). 20 wk-old male mice were used in all cases. Error bars: ± s.e.m. Data were analyzed pairwise with Student's unpaired T-test ***p<0.001 vs WT; **p<0.01 vs WT; $^{+++}$p<0.001 vs *Lmna*$^{H222P/H222P}$; $^{++}$p<0.01 vs *Lmna*$^{H222P/H222P}$. Scale bars: 25µm (**C**).

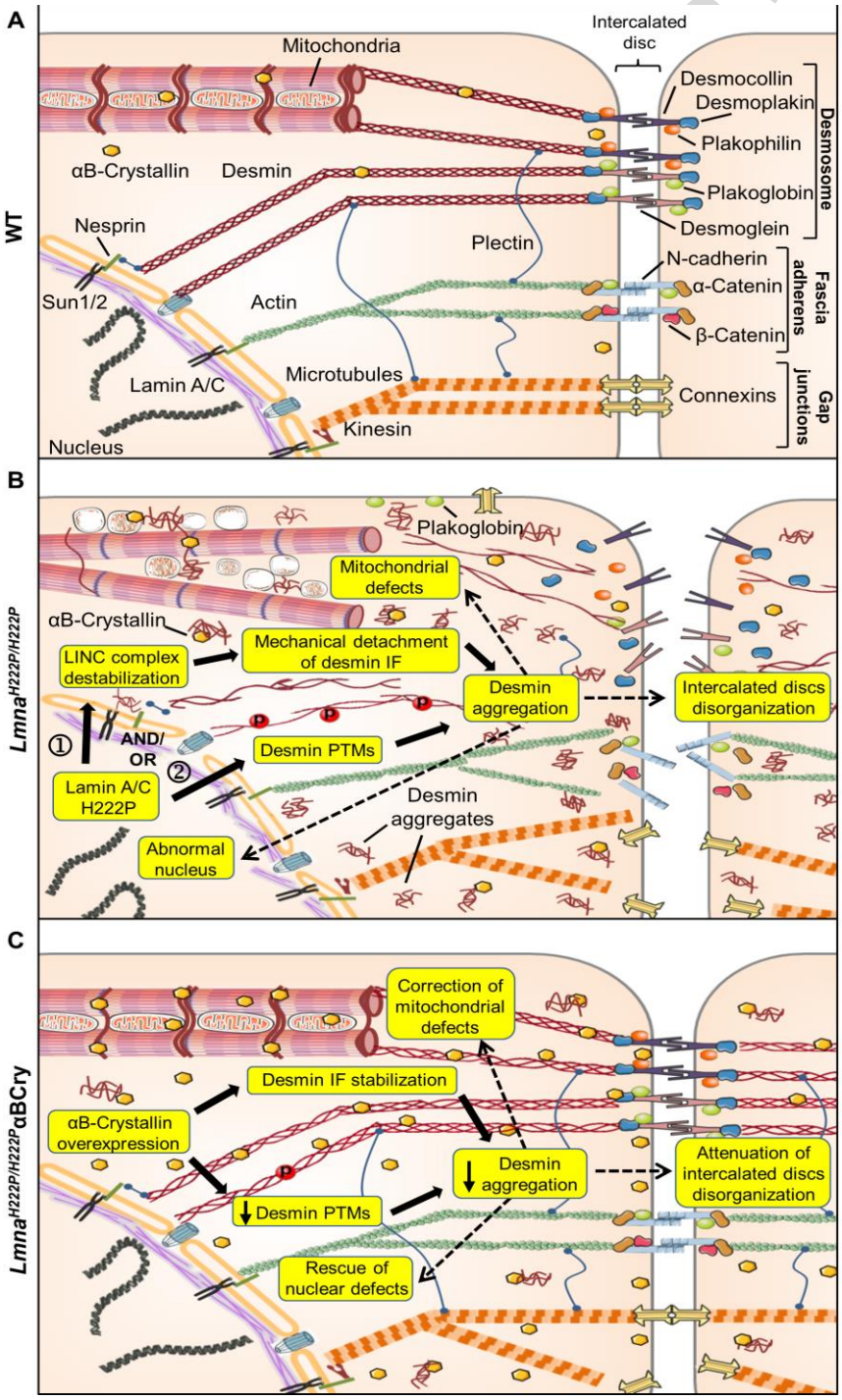

Fig.8. Schematic representation of the proposed desmin-dependent mechanism that contributes to the development of *Lmna*$^{H222P/H222P}$ cardiomyopathy. Desmin intermediate filament scaffold (in red) and its interactions with the major protein complexes found in the cardiac IDs and the nucleus. At the level of IDs, desmin interaction with desmoplakin facilitates the efficient targeting to desmosomes as well as their stabilization. In addition, the association of desmin with the nucleus through the LINC complexes or directly though the nuclear pores provides the physical and functional coupling between the cytoplasm and the nuclear interior. Desmin network interactions that interlink the contractile apparatus with costameres and different organelles (e.g. mitochondria and sarcoplasmic reticulum [26]) as well as several other desmin-associated proteins are not shown (**A**). In our proposed model, the mutant lamin A/C induces desmin network disruption and aggregation either by destabilization of LINC complexes ①, leading to mechanical detachment of desmin IFs and/or by inducing stresses leading to increased desmin PTMs (e.g. phosphorylation) ② causing its aggregation. These aggregates compromise proper targeting of desmoplakin (in blue) to the desmosomes and consequently their stabilization, thus also affecting indirectly the stability of fascia adherens and gap junctions and their components. In addition, or alternatively, desmin network destabilization could influence, through the linker plectin, the other two cytoskeletal networks, actin microfilaments and microtubules, thus contributing to the observed mislocalization of plakoglobin (in green) or connexin-43 (in yellow), consistent with the previously reported effects in actin [46] and microtubule[47, 48] cytoskeleton in the *Lmna*$^{H222P/H222P}$ mouse cardiomyocytes. Similarly, desmin network destabilization and aggregation leads to the expected mitochondrial defects due to loss of proper desmin function[26] (**B**). The overexpressed αBCry in *Lmna*$^{H222P/H222P}$ cardiomyocytes associates with desmin to prevent its misfolding and abnormal aggregation and ameliorates the desmin-dependent mislocalization of basic ID protein components as well as the mitochondrial and nuclear abnormalities (**C**).

4. Discussion

4.1. Desmin network disruption, disorganization of IDs and mitochondrial defects as a mechanism contributing to the progression of *Lmna*$^{H222P/H222P}$ cardiomyopathy.

Several converging lines of evidence have suggested that the link between desmin and lamins serves as a major integrator point for the intracellular communication between the nucleus and the rest of the cell[2-4, 6]. We demonstrated that the proper organization of desmin network is severely affected in *Lmna*$^{H222P/H222P}$ mice hearts as desmin loses its normal Z disk and ID localization pattern and accumulates into cytoplasmic aggregates. It is worth to mention that in *Lmna*$^{H222P/H222P}$ hearts the extent of desmin mislocalization and aggregate formation correlates with the heart function, as indicated by immunofluorescence analysis. Specifically, in mice that have been examined through echocardiography and exhibited severe cardiac dysfunction, the aberrant desmin staining pattern was more pronounced and frequent compared to animals which have moderate or milder cardiac pathology (Fig. S2). These findings are in line with previously published observations which have shown that lamin A/C deficiency leads to desmin filament detachment from the nuclear surface[30, 31] and disorganization[31, 49]. In addition, nuclear shape and positioning were altered in cardiac muscle of *Des-/-* mice[50]. Furthermore, in the hearts of *Lmna*$^{N195K/N195K}$ mice, another genetically engineered model of DCM with conduction system disease, though aggregate formation was not reported, desmin displayed a less organized immunofluorescence staining at the sarcomeres and the IDs[51].

As the *Lmna*$^{H222P/H222P}$ model mimics the clinical features of human DCM development in laminopathic patients[32], it was important to address potential mechanisms by which the observed desmin network defects in these cardiomyocytes contribute to the disease progression. We revealed that in *Lmna*$^{H222P/H222P}$ hearts, basic protein components of the IDs, such as desmoplakin, plakoglobin and connexin-43 are mislocalized and present abnormal intracellular deposition, thus suggesting for the first time a mechanism by which a nuclear protein could cause desmin-mediated conduction system defects (Fig. 8). Importantly, desmoplakin, the direct desmin-binding partner, exhibits the most severe type of mislocalization. Probably, the defective desmin network in *Lmna*$^{H222P/H222P}$ hearts hampers the interaction between desmin and desmoplakin and affects the proper targeting and

localization of the latter resulting in the destabilization of desmosomes. This is consistent with previous studies which have suggested that the assembly state of desmin affects its binding to desmoplakin[52] and also that mutations in desmoplakin gene cause loss of desmin from the IDs[53]. In addition, in epithelial cells proper localization of desmoplakin to desmosomes requires intact keratin IFs[54]. We showed that plakoglobin, which is found in both fascia adherens junctions and desmosomes, is also affected by the desmin network abnormalities but to lower extent, suggesting an additional desmin-independent targeting process for this protein to the "area composita" (adherens junctions and desmosomes). The dependence of the mislocalization pattern of critical components of the "area composita" and the ID defects to disrupted desmin network was confirmed by the significant restoration of these defects in *Lmna*$^{H222P/H222P}$αBCry and in *Lmna*$^{H222P/H222P}$*Des+/-* hearts, in which desmin aggregate formation was decreased. Regarding the gap junction structures in *Lmna*$^{H222P/H222P}$ hearts, we revealed that connexin-43 exhibits a severely disorganized staining pattern which is only partially corrected in *Lmna*$^{H222P/H222P}$αBCry and *Lmna*$^{H222P/H222P}$*Des+/-* hearts. Similar differences between connexin-43 and the other two ID proteins have been reported in the TNF-α model of HF, also linked to desmin disturbances[55]. In addition, numerous studies support the notion of a molecular crosstalk between mechanical and electrical coupling in cardiac muscle. Both the distribution and function of gap junction protein connexin-43 depends on the presence of sufficient mechanical stabilization of the ID by intact desmosomes and/or fascia adherens junctions [56, 57]. Importantly, this interdependence seems to be unilateral in the sense that the absence of connexin-43 does not seem to change the structure of adherens junctions and desmosomes[58]. Recent studies also showed that connexin-43 undergoes extensive remodeling with altered distribution ("lateralization") and decreased expression in *Lmna*$^{H222P/H222P}$ hearts implicating in these processes either the abnormal WNT/beta-catenin signaling and/or alterations of the microtubule cytoskeleton[47, 48]. In our present study, connexin-43 does not seem decreased but only mislocalized (Fig. 2Bb) but this slight discrepancy may be due to the different antibodies used for the immuno-localization of connexin-43. Therefore, we could speculate that connexin-43 targeting and stabilization to gap junctions is less desmin and more microtubule-dependent. In this context, we suggest that the amelioration of desmin network defects in *Lmna*$^{H222P/H222P}$αBCry and *Lmna*$^{H222P/H222P}$*Des+/-* hearts might stabilize directly the desmosomes of the "area composita" and consequently, the aforementioned crosstalk between mechanical and electrical coupling could partially reverse the redistribution of connexin-43.

Our results demonstrated that the *Lmna*$^{H222P/H222P}$ dilated cardiomyopathy is mainly caused by disruption and aggregation of the desmin network (Fig. 8). However, the mechanism by which the mutant lamin A/C induces desmin network disruption remains elusive. This is consistent with the mechanism proposed for *Lmna* deficiency[30, 31], most possibly, just detachment of desmin filaments from the nuclear membrane could cause a network collapse similarly to plectin deficiency[59]. This abnormal desmin aggregation could in turn affect the proper ID component targeting and consequently ID structure, thus leading to conduction and other cardiac defects. Importantly, we believe that desminopathy might be a major mechanism mediating every HF phenotype, given that, in most cases investigated, desmin network disruption is linked to deleterious consequences in mitochondria and IDs leading to cardiomyocyte death. In fact, changes in the distribution of ID proteins and/or desmin network defects have been described in several other models of cardiomyopathy, including the transverse aortic constriction (TAC)[60, 61] in addition to other models of the disease such as the HF mouse model with overexpression of TNF-α[55] or Myozap[62], as well as the coxsackievirus B3 induced HF[63]. In this context, it is believed that aberrant desmin network could be a common defect that mediates the development of cardiomyopathy independently of the mutated protein or the causative stimuli. Desmin network defects apart from their negative impact on the proper mitochondria and ID component targeting and consequently their structure and function, could result also to a generalized IF's network dysfunction that may affect the coupling between the cytoskeleton and the nucleus, the proper crosstalk between organelles and mechanotransduction. Given the linkage of IF

cytoskeleton to actin microfilaments and microtubules though plectin at least, it is not surprising to link their defects to the pathology of the *Lmna*$^{H222P/H222P}$[46-48] or TAC[61] mouse models of cardiomyopathy.

We also revealed that in *Lmna*$^{H222P/H222P}$ hearts desmin exhibits a different PTM status, as indicated by the presence of more acidic desmin isoforms in 2-D Western blot, compatible with increased phosphorylation. It is known that desmin is a substrate for a wide spectrum of PTMs such as phosphorylation, ADP-ribosylation, ubiquitination, glycation, oxidation and nitration[2, 37]. Normal phosphorylation levels of desmin control the dynamic assembly-disassembly of desmin filaments and potentially regulation of association with its binding partners[37]. On the other hand, desmin hyper-phoshorylation has been proposed as a mechanism of desmin filament disassembly and aggregate formation in cardiac disease[37-40]. Thus, we can speculate that the hyper-phosphorylation of desmin in *Lmna*$^{H222P/H222P}$ hearts may represent one potential mechanism that contributes to the deregulation of desmin network dynamics leading to desmin accumulation and aggregate formation. In support of this mechanism, previous data from *Lmna*$^{H222P/H222P}$ mice emphasized that there is a perturbation in multiple cellular signaling cascades with an increased activation status of a number of kinases such as the mitogen-activated protein kinase (MAPK) branches ERK1/2[43-45], Jun N-terminal kinase (JNK)[44] and p38α[64] as well as the AKT-mammalian target of rapamycin (mTOR)[65]. This hyper-activation of kinases in *Lmna*$^{H222P/H222P}$ hearts may indicate a generally perturbed stoichiometric balance towards increased phosphorylation events in many different protein substrates including probably desmin. In addition, considering that in *Lmna*$^{H222P/H222P}$ mouse hearts autophagy is impaired[65], defective protein quality control might also contributes to the accumulation of misfolded and/or phosphorylated desmin protein into cytoplasmic aggregates.

It has been shown that lamin A/C can serve as a nuclear docking platform for substrates of the ERK1/2 pathway[66]. In addition, cytoplasmic IFs can regulate signal transduction, potentially by serving as scaffold for signaling molecules[67]. For example, previous studies have documented a direct relationship between vimentin and ERK signaling in cancer cells and neurons[68]. In addition, the keratin 8 and 18 (K8/K18) IF proteins can regulate the ERK1/2 pathway by modulating the levels of c-Flip in epithelial cells[69]. Based on that, we could speculate that the fine-tuning of ERK1/2 signaling may be regulated, at least partially, through the cellular scaffold formed by desmin and desmin-associated proteins. Hence, the observed desmin network defects in *Lmna*$^{H222P/H222P}$ hearts could disrupt a potential cytoplasmic docking platform crucial for regulation of ERK1/2 pathway contributing to the aberrant activation of ERK1/2, either *per se* or in combination with the adverse effects of the mutant lamin A/C on this pathway. This hypothesis is further supported by our results indicating that the decreased desmin accumulation and aggregate formation in both *Lmna*$^{H222P/H222P}$αBCry and *Lmna*$^{H222P/H222P}$*Des*+/- hearts resulted in a significant amelioration of the aberrant ERK1/2 activation. We cannot exclude the possibility that desmin aggregation is both the consequence of an abnormal kinase activation cascade as well as the cause of this activation, or at least its maintenance through a feedback loop.

Additionally, since female *Lmna*$^{H222P/H222P}$ mice have not been included in this study as they develop later onset cardiomyopathy relative to male mice [32], the consequences of desmin network defects in these mice might be different, allowing a longer disease-free survival. Although we cannot rule out such a cause, previous data from *Lmna*$^{H222P/H222P}$ mice hearts have indicated that the nuclear accumulation of androgen receptor (AR) and the role of sex hormones associate with the observed gender differences in *LMNA* cardiomyopathy[70].

4.2. αBCry overexpression as a very attractive therapeutic strategy for lamin A/C/Desmin linked cardiomyopathies.

In the present study we describe the rescue of *Lmna*$^{H222P/H222P}$ cardiac pathology by ameliorating desmin network defects. We revealed that the cardiac-specific overexpression of the chaperone protein αBCry confers cardioprotection and improvement of the *Lmna*$^{H222P/H222P}$ heart function by reducing desmin accumulation and aggregate formation, by

attenuating the mislocalization of ID protein components and by rescuing mitochondrial defects (Fig. 8). It also improves some of the most well-documented pathological features of *Lmna*$^{H222P/H222P}$ mice such as the heart fibrosis, the abnormal nuclear elongation of cardiomyocytes and the aberrant activation of the ERK1/2 signaling pathway. Besides the well-established chaperone role of αBCry in preventing abnormal protein aggregation[23-25], αBCry acts as an important regulator of cytoprotection against various forms of cellular stress in the heart, most possibly, also through its chaperone activity. It is important to note that the extensive cardioprotective effects of αBCry overexpression, both in the presence of desmin aggregation described herein, as well as in its complete absence, demonstrated with the desmin null cardiomyopathy[26], strongly suggests that it protects against all defects caused by loss of desmin function, in addition to the gain of toxic aggregate function. As discussed above, mitochondrial defects are the earliest observed defects in desmin null hearts, leading to oxidative stress, cardiomyocyte death, inflammation and fibrosis, pathologies that are extensively ameliorated by αBCry overexpression[26]. All the above can explain the independently shown protection by αBCry overexpression against ischemia/reperfusion injury, cell death, redox imbalance and inflammation in the heart[71, 72]. Nevertheless, we do not exclude the possibility that the overexpressed αBCry might also directly affect beneficially other aspects of *Lmna*$^{H222P/H222P}$ cardiac pathology, independently of the desmin aggregation, as it could be in the case of the desmin null cardiomyopathy[26].

The major role of desmin aggregation in the generation of the *LMNA* cardiomyopathy, was further supported by the consequences of the reduced endogenous desmin protein levels in the *Lmna*$^{H222P/H222P}$*Des*+/- mice. We showed that in these hearts there is a significant amelioration of desmin aggregate formation along with a concomitant relocation of ID protein components, consistent with the improved cardiac function. This finding was indeed better than expected given that in *Des*+/- cardiomyocytes the amount of the protein is only 50% less than in the *Des*+/+ with all the herein described *Lmna*$^{H222P/H222P}$ pathology. In addition, despite the decrease of desmin to half amount of WT levels, the H222P *Lmna* gene mutation is able to increase the desmin accumulation to 3.3 fold in *Lmna*$^{H222P/H222P}$*Des*+/- versus 5.6 fold in *Lmna*$^{H222P/H222P}$*Des*+/+ (herein referred to *Lmna*$^{H222P/H222P}$*).* This data strongly suggested that this 50% difference was very critical for the development of the pathology. On the other hand, the results with the *Lmna*$^{H222P/H222P}$αBCry hearts strongly demonstrated that the αBCry overexpression in *Lmna*$^{H222P/H222P}$ mouse hearts provided the highest level of cardioprotection, as supported by our previous studies with desmin null mice[26]. On the other hand, the reduced desmin protein levels of *Lmna*$^{H222P/H222P}$*Des*+/- mice do show reduction of total heart fibrosis but the changes are not statistically significant due to big variations between samples. Nevertheless, there are several issues that can explain the observed differences in fibrosis reduction levels due to αBCry overexpression in *Lmna*$^{H222P/H222P}$ mice than just reduction of desmin and consequently desmin aggregates. As we discussed above, the present data suggest that desmin defects are a major mechanism that contributes to the development of cardiomyopathy, however, it is not the only causative mechanism, particularly in a laminopathy mouse model like *Lmna*$^{H222P/H222P}$ which has potentially additional, desmin-independent adverse effects originating from the nucleus of cardiomyocytes, or non-cardiomyocytes, that could eventually stimulate inflammation and fibrosis. Therefore, the reduced endogenous desmin protein levels of *Lmna*$^{H222P/H222P}$*Des*+/- mice do reduce desmin aggregates and the consequent defects and cell death, but do not eliminate completely cell death, the major trigger of inflammation and fibrosis, or the corresponding desmin-independent stimuli. Indeed, previous studies indicated that the development of fibrosis in *Lmna*$^{H222P/H222P}$ hearts, was mediated by the increased expression of the connective tissue growth factor (CTGF/CCN2), a matricellular protein, which was triggered by the elevating transforming growth factor (TGF)-β/Smad signaling[42]. Obviously, the αBCry overexpression in *Lmna*$^{H222P/H222P}$ mice provides the highest level of cardioprotection because in addition to minimizing the desmin aggregates, it directly prevents the remaining desmin-dependent or independent defects as well[26].

5. Conclusions

We unveiled the pathogenic role of desmin cytoskeletal network defects in *Lmna*$^{H222P/H222P}$ cardiac pathology suggesting that a DCM linked laminopathy, caused by at least the *Lmna*$^{H222P/H222P}$ gene mutation, can mirror the pathological hallmarks of a desminopathy. Most importantly, we demonstrated that the overexpression of αBCry in *Lmna*$^{H222P/H222P}$ hearts confers significant cardioprotection in this laminopathy/desminopathy DCM model strongly suggesting that this therapeutic approach could be beneficial to other laminopathies with similar desminopathic hallmarks, without excluding the possibility of high benefit for cases like desmin null hearts, free of desmin aggregates, but with most downstream common defects, particularly the mitochondrial ones.

Glossary:

IFs	Intermediate filaments
αBCry	αB-Crystallin
IDs	Intercalated discs
DCM	Dilated cardiomyopathy
HF	Heart failure
PTMs	Post translational modifications
ERK1/2	Extracellular signal-regulated kinase 1/2
JNK	Jun N-terminal kinase
mTOR	mammalian target of rapamycin

Acknowledgements

We are grateful to L. Margaritis for his enormous help with Electron Microscopy, S. Pagkakis and E. Rigana for their help with confocal imaging and E. Mavroidis and S. Psarras for constant assistance throughout this work.

Sources of funding

This work was supported by ESPA 09SYN-21- 965 and ‘’Excellence II’’ ARISTEIA II 5342 grants from the Greek Secretariat for R&D to YC.

Disclosures

There are no disclosures.

Appendix A.

Supplementary data.

References

[1] Capetanaki Y, Bloch RJ, Kouloumenta A, Mavroidis M, Psarras S. Muscle intermediate filaments and their links to membranes and membranous organelles. Exp Cell Res. 2007;313:2063-76.

[2] Capetanaki Y, Papathanasiou S, Diokmetzidou A, Vatsellas G, Tsikitis M. Desmin related disease: a matter of cell survival failure. Current Opinion in Cell Biology. 2015;32:113-20.

[3] Swift J, Ivanovska IL, Buxboim A, Harada T, Dingal PC, Pinter J, et al. Nuclear lamin-A scales with tissue stiffness and enhances matrix-directed differentiation. Science. 2013;341:1240104.

[4] Georgatos SD, Weber K, Geisler N, Blobel G. Binding of two desmin derivatives to the plasma membrane and the nuclear envelope of avian erythrocytes: evidence for a conserved site-specificity in intermediate filament-membrane interactions. Proc Natl Acad Sci U S A. 1987;84:6780-4.

[5] Cattin ME, Muchir A, Bonne G. 'State-of-the-heart' of cardiac laminopathies. Current opinion in cardiology. 2013;28:297-304.

[6] Ho CY, Jaalouk DE, Vartiainen MK, Lammerding J. Lamin A/C and emerin regulate MKL1-SRF activity by modulating actin dynamics. Nature. 2013;497:507-11.

[7] Capetanaki Y. Desmin cytoskeleton: a potential regulator of muscle mitochondrial behavior and function. Trends in cardiovascular medicine. 2002;12:339-48.

[8] Lin F, Worman HJ. Structural organization of the human gene encoding nuclear lamin A and nuclear lamin C. The Journal of biological chemistry. 1993;268:16321-6.

[9] Turgay Y, Eibauer M, Goldman AE, Shimi T, Khayat M, Ben-Harush K, et al. The molecular architecture of lamins in somatic cells. Nature. 2017;543:261-4.

[10] Choi JC, Worman HJ. Nuclear envelope regulation of signaling cascades. Advances in experimental medicine and biology. 2014;773:187-206.

[11] Athirasala A, Hirsch N, Buxboim A. Nuclear mechanotransduction: sensing the force from within. Curr Opin Cell Biol. 2017;46:119-27.

[12] Worman HJ, Bonne G. "Laminopathies": a wide spectrum of human diseases. Exp Cell Res. 2007;313:2121-33.

[13] Dellefave L, McNally EM. The genetics of dilated cardiomyopathy. Current opinion in cardiology. 2010;25:198-204.

[14] Captur G, Arbustini E, Bonne G, Syrris P, Mills K, Wahbi K, et al. Lamin and the heart. Heart. 2018;104:468-79.

[15] McLendon PM, Robbins J. Desmin-related cardiomyopathy: an unfolding story. American journal of physiology Heart and circulatory physiology. 2011;301:H1220-8.

[16] van Spaendonck-Zwarts KY, van Hessem L, Jongbloed JD, de Walle HE, Capetanaki Y, van der Kooi AJ, et al. Desmin-related myopathy. Clinical genetics. 2011;80:354-66.

[17] Wang X, Robbins J. Heart failure and protein quality control. Circ Res. 2006;99:1315-28.

[18] Clemen CS, Herrmann H, Strelkov SV, Schroder R. Desminopathies: pathology and mechanisms. Acta neuropathologica. 2013;125:47-75.

[19] Tsikitis M, Galata Z, Mavroidis M, Psarras S, Capetanaki Y. Intermediate filaments in cardiomyopathy. Biophysical reviews. 2018;10:1007-31.

[20] Wang X, Osinska H, Klevitsky R, Gerdes AM, Nieman M, Lorenz J, et al. Expression of R120G-alphaB-crystallin causes aberrant desmin and alphaB-crystallin aggregation and cardiomyopathy in mice. Circ Res. 2001;89:84-91.

[21] Vicart P, Caron A, Guicheney P, Li Z, Prevost MC, Faure A, et al. A missense mutation in the alphaB-crystallin chaperone gene causes a desmin-related myopathy. Nature genetics. 1998;20:92-5.

[22] Maloyan A, Sanbe A, Osinska H, Westfall M, Robinson D, Imahashi K, et al. Mitochondrial dysfunction and apoptosis underlie the pathogenic process in alpha-B-crystallin desmin-related cardiomyopathy. Circulation. 2005;112:3451-61.

[23] Bennardini F, Wrzosek A, Chiesi M. Alpha B-crystallin in cardiac tissue. Association with actin and desmin filaments. Circ Res. 1992;71:288-94.

[24] Wang X, Klevitsky R, Huang W, Glasford J, Li F, Robbins J. AlphaB-crystallin modulates protein aggregation of abnormal desmin. Circ Res. 2003;93:998-1005.

[25] Sharma S, Conover GM, Elliott JL, Der Perng M, Herrmann H, Quinlan RA. alphaB-crystallin is a sensor for assembly intermediates and for the subunit topology of desmin intermediate filaments. Cell stress & chaperones. 2017;22:613-26.

[26] Diokmetzidou A, Soumaka E, Kloukina I, Tsikitis M, Makridakis M, Varela A, et al. Desmin and αB-crystallin interplay in the maintenance of mitochondrial homeostasis and cardiomyocyte survival. Journal of Cell Science. 2016;129:3705-20.

[27] Milner DJ, Taffet GE, Wang X, Pham T, Tamura T, Hartley C, et al. The absence of desmin leads to cardiomyocyte hypertrophy and cardiac dilation with compromised systolic function. J Mol Cell Cardiol. 1999;31:2063-76.

[28] Li Z, Colucci-Guyon E, Pincon-Raymond M, Mericskay M, Pournin S, Paulin D, et al. Cardiovascular lesions and skeletal myopathy in mice lacking desmin. Developmental biology. 1996;175:362-6.

[29] Milner DJ, Weitzer G, Tran D, Bradley A, Capetanaki Y. Disruption of muscle architecture and myocardial degeneration in mice lacking desmin. J Cell Biol. 1996;134:1255-70.

[30] Nikolova V, Leimena C, McMahon AC, Tan JC, Chandar S, Jogia D, et al. Defects in nuclear structure and function promote dilated cardiomyopathy in lamin A/C-deficient mice. J Clin Invest. 2004;113:357-69.

[31] Jahn D, Schramm S, Schnolzer M, Heilmann CJ, de Koster CG, Schutz W, et al. A truncated lamin A in the Lmna -/- mouse line: implications for the understanding of laminopathies. Nucleus. 2012;3:463-74.

[32] Arimura T, Helbling-Leclerc A, Massart C, Varnous S, Niel F, Lacene E, et al. Mouse model carrying H222P-Lmna mutation develops muscular dystrophy and dilated cardiomyopathy similar to human striated muscle laminopathies. Hum Mol Genet. 2005;14:155-69.

[33] Diokmetzidou A, Tsikitis M, Nikouli S, Kloukina I, Tsoupri E, Papathanasiou S, et al. Strategies to Study Desmin in Cardiac Muscle and Culture Systems. Methods in enzymology. 2016;568:427-59.

[34] Papathanasiou S, Rickelt S, Soriano ME, Schips TG, Maier HJ, Davos CH, et al. Tumor necrosis factor-α confers cardioprotection through ectopic expression of keratins K8 and K18. Nature Medicine. 2015;21:1076-84.

[35] Franke WW, Borrmann CM, Grund C, Pieperhoff S. The area composita of adhering junctions connecting heart muscle cells of vertebrates. I. Molecular definition in intercalated disks of cardiomyocytes by immunoelectron microscopy of desmosomal proteins. European journal of cell biology. 2006;85:69-82.

[36] Sheikh F, Ross RS, Chen J. Cell-cell connection to cardiac disease. Trends in cardiovascular medicine. 2009;19:182-90.

[37] Winter DL, Paulin D, Mericskay M, Li Z. Posttranslational modifications of desmin and their implication in biological processes and pathologies. Histochemistry and cell biology. 2014;141:1-16.

[38] Agnetti G, Halperin VL, Kirk JA, Chakir K, Guo Y, Lund L, et al. Desmin modifications associate with amyloid-like oligomers deposition in heart failure. Cardiovascular Research. 2014;102:24-34.

[39] Rainer PP, Dong P, Sorge M, Fert-Bober J, Holewinski RJ, Wang Y, et al. Desmin Phosphorylation Triggers Preamyloid Oligomers Formation and Myocyte Dysfunction in Acquired Heart Failure. Circ Res. 2018.

[40] Caron A, Chapon F. Desmin phosphorylation abnormalities in cytoplasmic body and desmin-related myopathies. Muscle & nerve. 1999;22:1122-5.

[41] Subramaniam A, Jones WK, Gulick J, Wert S, Neumann J, Robbins J. Tissue-specific regulation of the alpha-myosin heavy chain gene promoter in transgenic mice. The Journal of biological chemistry. 1991;266:24613-20.

[42] Chatzifrangkeskou M, Le Dour C, Wu W, Morrow JP, Joseph LC, Beuvin M, et al. ERK1/2 directly acts on CTGF/CCN2 expression to mediate myocardial fibrosis in cardiomyopathy caused by mutations in the lamin A/C gene. Human Molecular Genetics. 2016;25:2220-33.

[43] Muchir A, Shan J, Bonne G, Lehnart SE, Worman HJ. Inhibition of extracellular signal-regulated kinase signaling to prevent cardiomyopathy caused by mutation in the gene encoding A-type lamins. Hum Mol Genet. 2009;18:241-7.

[44] Muchir A, Pavlidis P, Decostre V, Herron AJ, Arimura T, Bonne G, et al. Activation of MAPK pathways links LMNA mutations to cardiomyopathy in Emery-Dreifuss muscular dystrophy. J Clin Invest. 2007;117:1282-93.

[45] Wu W, Iwata S, Homma S, Worman HJ, Muchir A. Depletion of extracellular signal-regulated kinase 1 in mice with cardiomyopathy caused by lamin A/C gene mutation partially prevents pathology before isoenzyme activation. Hum Mol Genet. 2014;23:1-11.

[46] Chatzifrangkeskou M, Yadin D, Marais T, Chardonnet S, Cohen-Tannoudji M, Mougenot N, et al. Cofilin-1 phosphorylation catalyzed by ERK1/2 alters cardiac actin dynamics in dilated cardiomyopathy caused by lamin A/C gene mutation. Hum Mol Genet. 2018;27:3060-78.

[47] Le Dour C, Macquart C, Sera F, Homma S, Bonne G, Morrow JP, et al. Decreased WNT/beta-catenin signalling contributes to the pathogenesis of dilated cardiomyopathy caused by mutations in the lamin a/C gene. Hum Mol Genet. 2017;26:333-43.

[48] Macquart C, Juttner R, Le Dour C, Chatzifrangkeskou M, Schmitt A, Gotthardt M, et al. Microtubule cytoskeleton regulates connexin 43 localization and cardiac conduction in cardiomyopathy caused by mutation in A-type lamins gene. Hum Mol Genet. 2018.

[49] Frock RL, Chen SC, Da DF, Frett E, Lau C, Brown C, et al. Cardiomyocyte-specific expression of lamin a improves cardiac function in Lmna-/- mice. PloS one. 2012;7:e42918.

[50] Capetanaki Y, Milner DJ, Weitzer G. Desmin in muscle formation and maintenance: knockouts and consequences. Cell structure and function. 1997;22:103-16.

[51] Mounkes LC, Kozlov SV, Rottman JN, Stewart CL. Expression of an LMNA-N195K variant of A-type lamins results in cardiac conduction defects and death in mice. Hum Mol Genet. 2005;14:2167-80.

[52] Lapouge K, Fontao L, Champliaud MF, Jaunin F, Frias MA, Favre B, et al. New insights into the molecular basis of desmoplakin- and desmin-related cardiomyopathies. J Cell Sci. 2006;119:4974-85.

[53] Yang Z, Bowles NE, Scherer SE, Taylor MD, Kearney DL, Ge S, et al. Desmosomal dysfunction due to mutations in desmoplakin causes arrhythmogenic right ventricular dysplasia/cardiomyopathy. Circ Res. 2006;99:646-55.

[54] Kroger C, Loschke F, Schwarz N, Windoffer R, Leube RE, Magin TM. Keratins control intercellular adhesion involving PKC-alpha-mediated desmoplakin phosphorylation. J Cell Biol. 2013;201:681-92.

[55] Panagopoulou P, Davos CH, Milner DJ, Varela E, Cameron J, Mann DL, et al. Desmin mediates TNF-alpha-induced aggregate formation and intercalated disk reorganization in heart failure. J Cell Biol. 2008;181:761-75.

[56] Saffitz JE. Dependence of electrical coupling on mechanical coupling in cardiac myocytes: insights gained from cardiomyopathies caused by defects in cell-cell connections. Annals of the New York Academy of Sciences. 2005;1047:336-44.

[57] Oxford EM, Musa H, Maass K, Coombs W, Taffet SM, Delmar M. Connexin43 remodeling caused by inhibition of plakophilin-2 expression in cardiac cells. Circ Res. 2007;101:703-11.

[58] Gutstein DE, Liu FY, Meyers MB, Choo A, Fishman GI. The organization of adherens junctions and desmosomes at the cardiac intercalated disc is independent of gap junctions. J Cell Sci. 2003;116:875-85.

[59] Konieczny P, Fuchs P, Reipert S, Kunz WS, Zeold A, Fischer I, et al. Myofiber integrity depends on desmin network targeting to Z-disks and costameres via distinct plectin isoforms. J Cell Biol. 2008;181:667-81.

[60] Wang X, Gerdes AM. Chronic pressure overload cardiac hypertrophy and failure in guinea pigs: III. Intercalated disc remodeling. J Mol Cell Cardiol. 1999;31:333-43.

[61] Wang X, Li F, Campbell SE, Gerdes AM. Chronic pressure overload cardiac hypertrophy and failure in guinea pigs: II. Cytoskeletal remodeling. J Mol Cell Cardiol. 1999;31:319-31.

[62] Frank D, Rangrez AY, Poyanmehr R, Seeger TS, Kuhn C, Eden M, et al. Mice with cardiac-restricted overexpression of Myozap are sensitized to biomechanical stress and develop a protein-aggregate-associated cardiomyopathy. J Mol Cell Cardiol. 2014;72:196-207.

[63] Ye X, Zhang HM, Qiu Y, Hanson PJ, Hemida MG, Wei W, et al. Coxsackievirus-induced miR-21 disrupts cardiomyocyte interactions via the downregulation of intercalated disk components. PLoS pathogens. 2014;10:e1004070.

[64] Muchir A, Wu W, Choi JC, Iwata S, Morrow J, Homma S, et al. Abnormal p38alpha mitogen-activated protein kinase signaling in dilated cardiomyopathy caused by lamin A/C gene mutation. Hum Mol Genet. 2012;21:4325-33.

[65] Choi JC, Muchir A, Wu W, Iwata S, Homma S, Morrow JP, et al. Temsirolimus activates autophagy and ameliorates cardiomyopathy caused by lamin A/C gene mutation. Sci Transl Med. 2012;4:144ra02.

[66] Gonzalez JM, Navarro-Puche A, Casar B, Crespo P, Andres V. Fast regulation of AP-1 activity through interaction of lamin A/C, ERK1/2, and c-Fos at the nuclear envelope. J Cell Biol. 2008;183:653-66.

[67] Eriksson JE, Dechat T, Grin B, Helfand B, Mendez M, Pallari HM, et al. Introducing intermediate filaments: from discovery to disease. J Clin Invest. 2009;119:1763-71.

[68] Virtakoivu R, Mai A, Mattila E, De Franceschi N, Imanishi SY, Corthals G, et al. Vimentin-ERK Signaling Uncouples Slug Gene Regulatory Function. Cancer research. 2015;75:2349-62.

[69] Gilbert S, Loranger A, Marceau N. Keratins modulate c-Flip/extracellular signal-regulated kinase 1 and 2 antiapoptotic signaling in simple epithelial cells. Molecular and cellular biology. 2004;24:7072-81.

[70] Arimura T, Onoue K, Takahashi-Tanaka Y, Ishikawa T, Kuwahara M, Setou M, et al. Nuclear accumulation of androgen receptor in gender difference of dilated cardiomyopathy due to lamin A/C mutations. Cardiovasc Res. 2013;99:382-94.

[71] Rajasekaran NS, Connell P, Christians ES, Yan LJ, Taylor RP, Orosz A, et al. Human alpha B-crystallin mutation causes oxido-reductive stress and protein aggregation cardiomyopathy in mice. Cell. 2007;130:427-39.

[72] Rothbard JB, Kurnellas MP, Brownell S, Adams CM, Su L, Axtell RC, et al. Therapeutic effects of systemic administration of chaperone alphaB-crystallin associated with binding proinflammatory plasma proteins. The Journal of biological chemistry. 2012;287:9708-21.

Graphical abstract

Highlights

- Desmin cytoskeletal network defects contributes to *Lmna*$^{H222P/H222P}$ cardiomyopathy
- Desmin network disruption leads to intercalated discs and mitochondrial defects
- A laminopathy can mirror the pathological hallmarks of a desminopathy
- Overexpression of αB-Crystallin confers cardioprotection in *Lmna*$^{H222P/H222P}$ mice
- Desmin-targeted treatment could be beneficial for *Lmna*$^{H222P/H222P}$ cardiomyopathy